

Performance Study and Energy Saving Process Analysis of Hybrid Absorption-Compression Refrigeration Cycles

Na Zhang¹

Institute of Engineering Thermophysics,
Chinese Academy of Sciences,
Beijing 100190, China
e-mail: zhangna@iet.cn

Noam Lior

Department of Mechanical Engineering and
Applied Mechanics,
University of Pennsylvania,
Philadelphia, PA 19104-6315
e-mail: lior@seas.upenn.edu

Wei Han

Institute of Engineering Thermophysics,
Chinese Academy of Sciences,
Beijing 100190, China
e-mail: hanwei@iet.cn

In an attempt to improve the performance of hybrid absorption and mechanical vapor compression refrigeration systems and to determine the fundamental reasons for such improvements, two configurations of the hybrid refrigeration cycle with a booster compressor at different positions of the cycle (between the evaporation and the absorber, or between the generator and the condenser) are simulated and analyzed. The interrelation between the two subcycles and the hybridization principle have been explored and clarified. An $\text{NH}_3/\text{H}_2\text{O}$ -based hybrid cycle is the basis of this simulation. It was found that (1) the hybrid cycle performance is mainly governed by the interaction between its two subcycles of mechanical compression and thermal compression and their respective energy efficiencies, and (2) the hybrid cycle primary energy-based coefficient of performance (COP) was higher by up to 15% (without internal heat recuperation) as compared with the nonhybrid absorption cycle, (3) in comparison with the nonhybrid absorption and vapor compression cycles working in the same temperature regions, the more efficient use of low-temperature heat by cascade utilization of the two energy inputs (heat rate and mechanical power) with different energy quality, and the enhanced refrigeration ability of low-temperature heat are the basic reasons for the hybrid cycle performance improvement and significant energy saving, (4) the hybrid cycle achieves an exergy efficiency of 36.5%, which is 27% higher than that of the absorption cycle, and 4.5% higher than the vapor compression cycle, achieving a thermal-driving exergy efficiency of 37.5% and mechanical work saving ratio up to 64%. [DOI: 10.1115/1.4034589]

Keywords: hybrid absorption-compression refrigeration cycles, low-temperature heat use, exergy and energy analysis, energy saving process

1 Introduction

Vapor compression is the most widely used technology for refrigeration, air conditioning, and heat-pump heating systems because of its relatively good performance and low capital cost. It, however, consumes the high-quality energy of electricity. As an alternative, the absorption cycle [1] has the potential of using low-temperature heat from a variety of sources such as waste heat recovery and solar and geothermal energy for refrigeration/cooling or heating applications. Such cycles may use one of a number of working fluids, with the lithium bromide aqueous solution (H_2O -LiBr) being the most common because of its favorable operation conditions for evaporation (and thus cooling) temperatures that are above 5°C [2]. The drawbacks of this working pair are the limitation of the working temperature range due to the freezing point of water and crystallization, and its corrosiveness for metal components of the machine at temperatures above 200°C [3]. Ammonia-water is another popular working solution especially for refrigeration. A comparison in Ref. [4] of four different working fluid pairs in single-effect absorption cycles concluded that the classical working pairs including H_2O -LiBr and NH_3 - H_2O offer the best combination of high-vaporization enthalpy of the refrigerant fluid and low solution circulation ratio (the ratio of the strong solution mass flow rate over the refrigerant mass flow rate). The coefficient of performance (COP) of

ammonia-water cycles is, however, low because of the need for rectification. One way to improve the COP of the single-effect absorption cycle is to integrate it with a mechanical compression process which consumes a small fraction ($\sim 10\%$ of the heat input) of mechanical work, and a system resulting from such hybridization is called as an absorption-compression hybrid cycle. Such a hybrid cycle was found [2,4] to consume less mechanical/electrical work as compared with the vapor compression cycle, and to have a higher COP than the absorption cycle, and has thus drawn significant attention in recent years.

Two basic configurations of such hybrid cycles were proposed: one with the compressor positioned between the evaporator and the absorber (at the cycle low-pressure side), and the other between the generator and the condenser (at the cycle high-pressure side) [5]. With different compressor positions and under different operation conditions, the hybrid cycle may offer some additional advantages besides the improved COP, such as increased absorption temperature, higher-temperature lift, or reduced generation temperature [4]. The reduction of generation temperature in an $\text{H}_2\text{O}/\text{LiBr}$ -based triple-effect absorption cooling system to avoid the corrosion problem was proposed in Ref. [3], where it was found that the generator temperature decrement increases as the compressor pressure ratio is raised, and that a 40°C generator temperature decrement can be obtained at the expense of 3–5% of cooling capacity equivalent power input for driving the compressor.

The same hybridization principle has been also applied in the generator absorber exchange (GAX) cycle, in which a part of the absorption-released heat is used as the complementary driving heat in the generator [6]. Such a compression-assisted GAX hybrid cycle with ammonia-water as working fluid was analyzed

¹Corresponding author.

Contributed by the Advanced Energy Systems Division of ASME for publication in the JOURNAL OF ENERGY RESOURCES TECHNOLOGY. Manuscript received October 31, 2015; final manuscript received August 9, 2016; published online September 14, 2016. Assoc. Editor: Vittorio Verda.

in Refs. [7,8], and it was found that 26–30% higher *COP* is achievable in the hybrid cycle.

In addition to the basic configurations, some new cycle configurations were also proposed for further improving the hybrid cycle performance [9–11]. With the cascade utilization of the input waste heat, the hybrid absorption–compression refrigeration system proposed by Han et al. generates 47% more cooling than the conventional absorption refrigeration cycle (AC) [11].

Most of the research in the hybrid cycles focused on the parametric analysis and selection of working solutions, and some on configuration development. Zheng and Meng explored the potential of lowering evaporation temperature in the absorption refrigeration cycle, and pointed out that the lowest evaporation temperature occurs at the thermodynamic ultimate state with infinitesimal concentration difference and infinite circulation ratio [12,13]. The energy saving process of the hybrid refrigeration cycle has also been discussed by comparing the trade-off effects of the compressor pressure on the subcycle performance, mainly based on the behavior change of the absorption cycle near its ultimate state.

Such a hybrid refrigeration cycle (using, however, steam-ejector for the compression) was proposed already in Ref. [14], and as described above, they were well studied since, but the understanding of the interactions between the two subcycles (absorption and mechanical compression cooling) and of their resulting energy saving process in the overall hybrid cycle, remains insufficient. The focal objective and contribution of this study is thus to improve this understanding of the interaction processes between the mechanical compression and thermal compression subprocesses using low-temperature (<150 °C) driving heat. To explore the thermodynamic performance and the energy saving processes of the hybrid cycle, an energy and exergy comparison study was also conducted among the hybrid cycles and the conventional vapor compression and absorption refrigeration cycles working within the same temperature regions, revealing more efficient use of low-temperature heat in the hybrid cycle by cascade utilization of the two energy inputs (heat rate and mechanical power) having different energy qualities. The study provided important new insights about the interrelationship between the two subcycles and quantitatively revealed the processes of energy saving in such hybrid cycles.

2 Configuration Description of the Hybrid Absorption-Compression Refrigeration Cycle

The single-effect absorption refrigeration cycle consists of a generator, condenser, evaporator and absorber, solution pump, heat exchanger, and throttling valves (in Figs. 1 and 2 without the compressor COMP). Taking advantage of the large boiling point

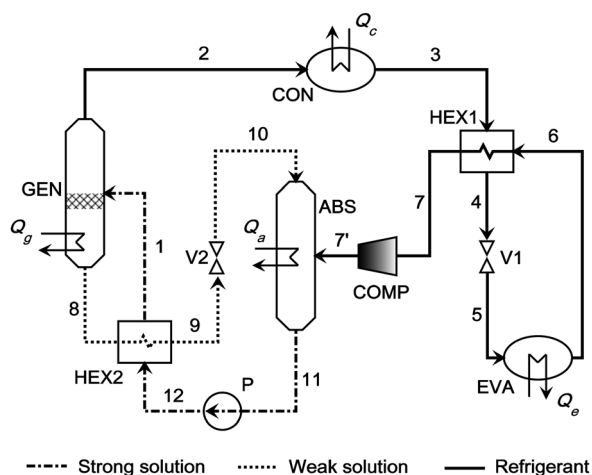


Fig. 1 Hybrid cycle with low-pressure-side compressor

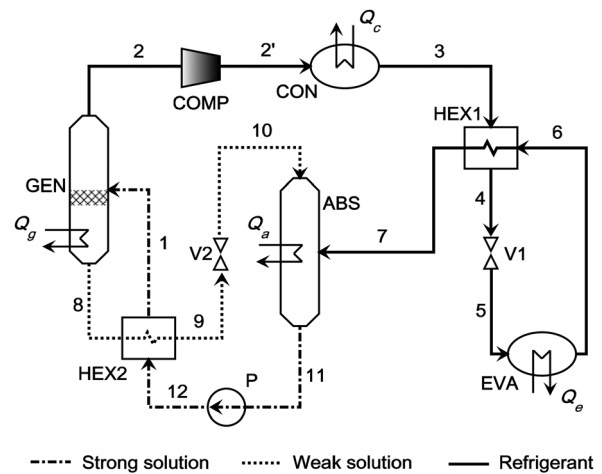


Fig. 2 Hybrid cycle with high-pressure-side compressor

difference between the refrigerant and the absorbent, the flow loops of the refrigerant ($1 \rightarrow 2 \rightarrow 3 \rightarrow 4 \rightarrow 5 \rightarrow 6 \rightarrow 7 \rightarrow 11$, solid line) and of the solution ($1 \rightarrow 8 \rightarrow 9 \rightarrow 10 \rightarrow 11 \rightarrow 12 \rightarrow 1$, dotted- and dotted-dash line) are formed, they separate in the generator (state points 2 and 8) and join together in the absorber (point 11). By arranging generation and condensation at a higher pressure, and evaporation and absorption at a lower pressure, the system has two pressure levels and three temperature levels (assuming $T_a = T_c$). Driven by the higher-temperature (T_g) heat Q_g in the generator, the system intakes lower-temperature (T_e) heat Q_e in the evaporator, which is the cooling/refrigeration objective, and delivers midtemperature (T_c) heat amounts Q_c and Q_a in the condenser and absorber, respectively.

The hybridization of the system is accomplished by integrating within it a compressor that compressed the same refrigerant used in the absorption cycle and thus boosts its pressure. As explained in Ref. [5], the compressor COMP can be positioned either between the evaporator and the absorber (at the low-pressure side, Fig. 1), or between the generator and the condenser (at the high-pressure side, Fig. 2). The hybrid cycle can, therefore, be regarded as a combination of thermal compression and mechanical compression. Such addition of a compressor thus adds one more operational option to the hybrid cycle by creating a medium pressure level in the hybrid cycle, which enables the hybrid cycle to be operated more flexible and achieve good performance over a wide operation range [4]. The thermodynamic diagrams of the first cycle (Fig. 1) are shown in Sec. 5 further below.

3 Simulation Method and Assumptions

3.1 The Thermodynamic Model and Its Validation.

Ammonia–water is a widely employed working solution especially for refrigeration purpose, and it is chosen to be the working solution in this study because of its proven performance for applications well-below the ambient temperature, and for its easy availability. The drawback of this working solution is the need for rectification, and that the presence of a small fraction of water vapor in the refrigerant may cause some operational problems in the ammonia compressor [2].

The simulations were carried out using the commercial Aspen Plus [15] program, in which the component models are based on energy, mass and species balances, with the default relative convergence error tolerance of 0.01%; the thermal properties were calculated with the thermal property method of the electrolyte nonrandom two-liquid model. To validate the properties calculations, the property results from Aspen Plus and the vapor–liquid equilibrium (VLE) data published by the International Institute of Refrigeration [16] were compared, and they were found to be in

good agreement: the absolute error of the water mass percentage in saturated NH₃/H₂O vapor was within 1%, and the average relative error in the boiling point temperature was ~2.6%.

Driving heat sources in the range of 100–150 °C such as industrial waste heat and solar and geothermal energy can thus be used. Some of the assumptions are:

- (1) Steady-state operation.
- (2) Relative (to the inlet pressure) pressure losses in the generator, condenser, evaporator, and absorber are 3%.
- (3) Expansion through the throttle valve is isenthalpic.
- (4) Heat losses to the ambient are ignored.
- (5) The outflow solutions of the generator and absorber are at saturated states.

The other assumptions, for the calculations, and major equipment specifications are summarized in Table 1.

The ammonia and H₂O mass balance and energy balances are established for each elementary component. The equations of energy balance and exergy destruction and loss for each component are as follows [11]:

Generator GEN

$$m_1 h_1 + Q_g = m_2 h_2 + m_8 h_8 \quad (1)$$

$$E_{D,GEN} = E_g + (m_1 h_1 - m_2 h_2 - m_8 h_8) - T_0(m_1 s_1 - m_2 s_2 - m_8 s_8) \quad (2)$$

Condenser CON

$$m_2 h_2 = m_3 h_3 + Q_c \quad (3)$$

$$E_{D,CON} = (m_2 h_2 - m_3 h_3) - T_0(m_2 s_2 - m_3 s_3) \quad (4)$$

Heat exchanger HEX1

$$m_3 h_3 + m_6 h_6 = m_4 h_4 + m_7 h_7 \quad (5)$$

$$E_{D,HEX1} = T_0(m_4 s_4 + m_7 s_7 - m_3 s_3 - m_6 s_6) \quad (6)$$

Valve V1

$$m_4 h_4 = m_5 h_5 \quad (7)$$

$$E_{D,V1} = T_0(m_5 s_5 - m_4 s_4) \quad (8)$$

Evaporator EVA

$$m_5 h_5 + Q_e = m_6 h_6 \quad (9)$$

$$E_{D,EVA} = (m_5 h_5 - m_6 h_6) - T_0(m_5 s_5 - m_6 s_6) - E_e \quad (10)$$

Absorber ABS

$$m_7 h_7 + m_{10} h_{10} = m_{11} h_{11} + Q_a \quad (11)$$

$$E_{D,ABS} = (m_7 h_7 + m_{10} h_{10} - m_{11} h_{11}) - T_0(m_7 s_7 + m_{10} s_{10} - m_{11} s_{11}) \quad (12)$$

Valve V2

$$m_9 h_9 = m_{10} h_{10} \quad (13)$$

$$E_{D,V2} = T_0(m_{10} s_{10} - m_9 s_9) \quad (14)$$

Pump *p*

$$m_{11} h_{11} + W_P = m_{12} h_{12} \quad (15)$$

$$E_{D,P} = T_0(m_{12} s_{12} - m_{11} s_{11}) \quad (16)$$

Heat exchanger HEX2

$$m_8 h_8 + m_{12} h_{12} = m_1 h_1 + m_9 h_9 \quad (17)$$

$$E_{D,HEX2} = T_0(m_1 s_1 + m_9 s_9 - m_8 s_8 - m_{12} s_{12}) \quad (18)$$

Compressor COMP

$$m_{in} h_{in} + W_C = m_{out} h_{out} \quad (19)$$

$$E_{D,COMP} = T_0(m_{out} s_{out} - m_{in} s_{in}) \quad (20)$$

The simulation model was validated by comparing with the available literature data from Ref. [11], in which a basic NH₃-H₂O absorption refrigeration cycle was simulated with the engineering equation solver (EES) software, and validated. Driven in their simulation by the exhaust gas at temperature of 350 °C, and with a generation temperature of 135 °C, an evaporation temperature of -15 °C, and refrigerant ammonia concentration of 0.998, they found that the cycle *COP* and exergy efficiency were 0.5 and 16.7%, respectively, and the refrigeration exergy production was 16.3 kW. In our ASPEN Plus simulation of the refrigeration cycle under the same conditions, the *COP* and exergy efficiency were found to be 0.49, and 16.3%, respectively, and the refrigeration exergy output was 16.0 kW. This comparison shows that the results agree very well, with relative errors within 2%.

3.2 Evaluation Criteria. The coefficient of performance (*COP*) based on the first law of thermodynamics is defined as

$$COP_0 = \frac{Q_e}{Q_g + W} \quad (21)$$

This definition is for both the absorption cycle (with *W* being the pump power consumption) and the hybrid cycle (with *W* being the sum of the pump and compressor power consumptions).

The two energy inputs, mechanical work *W*, and heat input *Q_g* to the generator, have very different energy qualities. To better account for the difference of the two energy inputs, the primary energy-based coefficient of performance is defined in Refs. [4,5] as

$$COP_p = \frac{Q_e}{Q_g + (W_p + W_c)/\eta_e} \quad (22)$$

where η_e is the electricity generation efficiency, and is assumed to be 40% as an average value for electricity production and delivery.

As defined in Eq. (22), the primary energy-based *COP_p* cannot differentiate between the heat inputs at different temperatures. Furthermore, it considers the energy of invested electricity in the same way as the heat energy, ignoring the fact that the electricity is typically generated by using heat at high-temperature of fossil fuel combustion. To properly account for the contribution from such different energy qualities, and to obtain further guidance for

Table 1 Specified simulation parameters of major components

Item	Value
Minimal temperature difference in the heat exchanger (HEX) (°C)	5
Pump efficiency	0.7
Compressor isentropic efficiency	0.7
Mass fraction of the H ₂ O in the refrigerant	<0.4%

improving system design, we also perform an exergy analysis and use also an exergy efficiency [17–19], defined here as:

$$\eta_{ex} = \frac{E_c}{E_g + W} \quad (23)$$

where E stands for exergy, calculated by:

$$E_c = Q_e(T_0/\bar{T}_e - 1) \quad (24)$$

$$E_g = Q_g(1 - T_0/\bar{T}_g) \quad (25)$$

where \bar{T}_g and \bar{T}_e are the average generation heat addition and evaporation temperatures, respectively.

4 Hybrid Cycle Simulations and Discussion of System Performance

4.1 Cycle Simulation and Performance Comparison. The advantages of the hybrid absorption–compression cycle was summarized by Boer [4]. Amongst them, a very desirable feature is its ability to operate efficiently with low driving temperatures, to be able to use low-temperature heat from waste and renewable energy sources.

This hybrid cycle performance with reduced driven heat temperature is investigated in this paper, for given evaporation and condensation pressure/temperature. In the hybrid cycle with low-pressure-side compressor (LC), elevating the absorption pressure allows the use of higher-strong solution concentration to maintain a constant absorption temperature. If the refrigerant mass flow rate remains the same, the weak solution concentration will increase too, resulting in a desirable drop of the generation

temperature T_g . For the hybrid cycle with a compressor at the high-pressure side (HC), this high-pressure-side compressor lowers the generation pressure. If the solution concentrations are kept the same, the generation temperature drops accordingly, thus allowing the use of lower temperature heat.

The two typical hybrid cycles, one with a low-pressure-side compressor and the other with a high-pressure-side compressor, are simulated for the same condensation and evaporation temperatures, and at the compressor pressure ratio $\pi = 2.5$. Other related assumptions are the same as in Table 1. For comparison, a nonhybrid absorption refrigeration cycle (AC) and a mechanical vapor compression cycle (VC) are also simulated, under the same conditions (the same working solution and concentrations, working temperature regions and component performance) as the hybrid cycles.

The parameters for the main states of the two hybrid cycles are shown in Tables 2 and 3. Table 4 summarizes the cycle performance comparison. With the same refrigerant mass flow rate, these four cycles produce the same rate of refrigeration, of 17 MW. The nonhybrid absorption cycle (AC) serves as a starting point and base for the comparison, with a generation pressure and temperature of 15.7 bar and 151.7 °C, and rich and weak solution concentrations of 30% and 17.7%, respectively, and the compressor pressure ratio π can be considered as 1.0, and the cycle was found to have a COP_p of 0.399. The vapor compression cycle (VC) serves as the other end of comparison, with a pressure ratio of 10.3, it consumes electricity and has a primary-energy-based COP_p of 0.7.

In the HC cycle, increasing the compressor pressure ratio to 2.5 causes the generation pressure to drop to 6.28 bar, leading to the drop of the generation temperature from 151.7 °C to 109 °C, and of the generation heat demand from 42 MW to 36.2 MW. Nevertheless, this drop of the generation heat demand cannot

Table 2 Main state parameters of the hybrid LC cycle

State	T (°C)	P (bar)	Vapor fraction	Mass flow rate (kg/s)	NH ₃ mass concentration x	h (kJ/kg)	s (kJ/(kg·K))
1	94	16.2	0	100	0.461	−10265.0	−9.215
2	70.3	15.7	1	15	0.996	−2674.0	−6.902
3	40	15.25	0	15	0.996	−3849.7	−10.670
4	15.1	14.9	0	15	0.996	−3991.9	−11.104
5	−23.7	1.605	0.149	15	0.996	−3991.9	−11.009
6	−15	1.557	0.98	15	0.996	−2858.0	−6.450
7	34.9	1.525	1	15	0.996	−2715.9	−5.933
7'	134.3	3.813	1	15	0.996	−2499.6	−5.768
8	109.1	15.7	0	85	0.367	−11297.8	−8.805
9	45.2	15.39	0	85	0.367	−11691.5	−9.857
10	45.3	3.813	0	85	0.367	−11691.5	−9.855
11	40	3.7	0	100	0.461	−10602.2	−10.139
12	40.3	16.5	0	100	0.461	−10599.7	−10.134

Table 3 Main state parameters of the hybrid HC cycle

State	T (°C)	P (bar)	Vapor fraction	Mass flow rate (kg/s)	NH ₃ mass concentration x	h (kJ/kg)	s (kJ/(kg·K))
1	86.9	6.474	0.016	100	0.3	−12213.9	−8.980
2	47.6	6.28	1	15	0.996	−2701.3	−6.562
2'	150	15.7	1	15	0.996	−2483.3	−6.402
3	40	15.25	0	15	0.996	−3850.0	−10.670
4	15.1	14.9	0	15	0.996	−3992.4	−11.105
5	−23.7	1.605	0.148	15	0.996	−3992.4	−11.009
6	−15	1.557	0.98	15	0.996	−2858.5	−6.451
7	34.9	1.525	1	15	0.996	−2716.2	−5.933
8	109	6.28	0	85	0.177	−13533.7	−8.444
9	45.2	6.154	0	85	0.177	−13864.7	−9.356
10	45.3	1.525	0	85	0.177	−13864.7	−9.355
11	40.1	1.48	0	100	0.3	−12496.2	−9.781
12	40.2	6.606	0	100	0.3	−12495.3	−9.779

Table 4 Performance comparison between the hybrid and non-hybrid cycles

	Hybrid LC	Hybrid HC	AC	VC
Compressor pressure ratio π	2.5	2.5	1.0	10.3
Compressor inlet temperature ($^{\circ}\text{C}$)	34.9	47.6	—	34.8
Compressor outlet temperature ($^{\circ}\text{C}$)	134.3	150	—	312
Absorption heat Q_a (MW)	28.94	30.38	30.43	—
Condensation heat Q_c (MW)	17.64	20.5	17.64	26.67
Energy input				
Q_g (MW)	28.32	36.16	41.99	—
W_p (MW)	0.245	0.090	0.26	—
W_c (MW)	3.245	3.270	—	9.676
Energy output (cooling)				
Q_e (MW)	17.0	17.0	17.0	17.0
COP_p	0.459	0.382	0.399	0.702

compensate for the compressor power consumption of 3.27 MW which, also has a much higher-energy quality (exergy), and thus, the hybrid cycle COP_p drops to 0.38, below that of the nonhybrid absorption cycle.

Increasing the compressor pressure ratio to 2.5 in the LC mode raises the absorption pressure to 3.7 bar. To maintain the same absorption temperature of 40°C , the strong solution concentration has to be raised to 46.1%. The generation pressure remains the same as that in the nonhybrid absorption cycle, thus, the weak solution concentration increases as well, here to 36.7%, leading to a drop of the generation temperature to 109°C . Apparently, the higher strong-solution concentration favors the generation (rectification) process, and the generation heat demand drops significantly, by 32.6%, from 42 MW to 28.3 MW and at the same time the compressor power consumption is merely 3.24 MW. The hybrid cycle has a much higher COP_p value of 0.46, 15% higher than the nonhybrid absorption cycle. The primary-energy-based COP_p undervalues, however, the benefits of the hybridization by ignoring the fact that the hybrid absorption cycle utilizes much lower temperature heat as compared with the nonhybrid absorption cycle.

The compressor inlet temperature is about $35\text{--}50^{\circ}\text{C}$, and the pressure ratio about 2–3. From the practical standpoint, the hybrid cycle does not pose serious technical obstacles since the ammonia compressor and the ammonia–water absorption refrigerator are very mature technologies. At the same time, while the integration with a compressor brings more operation flexibility, it also makes the system more complex and increases the system cost. The economic analysis of the hybrid cycle is of significant interest but is beyond the scope of the current study.

Assuming that the high-pressure-side compressor has a higher-inlet temperature, the authors of Ref. [12] concluded that the high-pressure-side compressor consumes more power than the low-pressure-side one, and attribute the hybrid cycle performance difference to this power consumption difference between the positioning of the compressor in the two cycles. We found in this study, however, that the compressor power consumptions are almost the same in LC and HC despite their different positions in the cycle, because the difference between their inlet temperatures is moderate. The major difference is in the heat demand of their generators, which confirms that the key to the success of hybridization is the improvement of the absorption subcycle performance.

4.2 Parameter Sensitivity Analysis. To provide further understanding of the hybridization, a study was conducted to compare in detail the performance for the two hybrid cycles as a function of the compressor pressure ratio π , and the results are summarized in Figs. 3–5. The calculation is performed for $T_c=40^{\circ}\text{C}$, the refrigerant is almost pure ammonia with the ammonia mass concentration of $\geq 99.6\%$, it produces refrigeration at a temperature of -23°C to -15°C in the evaporator. The

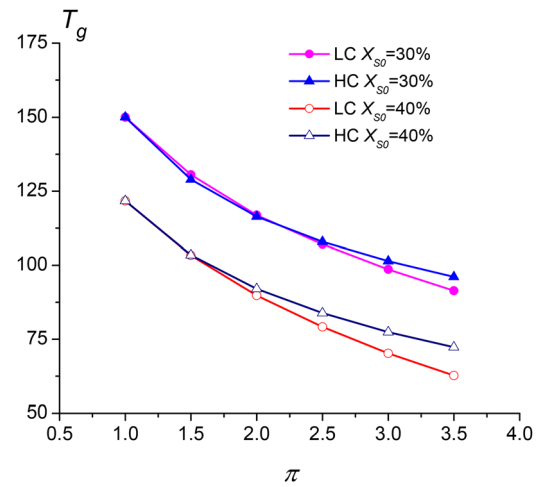


Fig. 3 Variation of the generation temperature T_g with the pressure ratio π

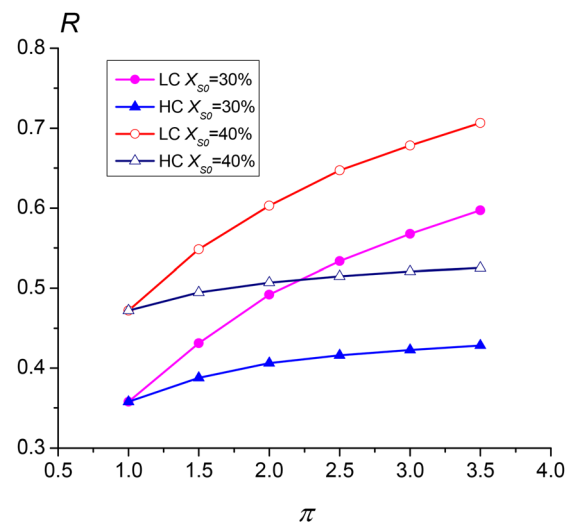


Fig. 4 Variation of R (refrigerant production)/(generator heat input) with the pressure ratio π

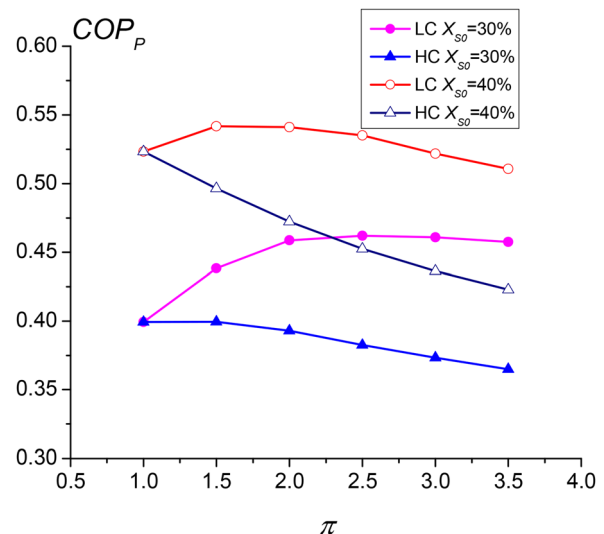


Fig. 5 Variation of the primary energy-based coefficient of performance COP_p with the pressure ratio π

calculation is based on 100 kg/s strong solution mass flow rate, and it is started with $\pi=1.0$, at which state $T_g=151.7^\circ\text{C}$, $T_c=T_a=40^\circ\text{C}$ for two basic strong solution concentrations, $x_{s0}=30\%$ and 40% .

Figure 3 shows the drop of T_g associated with increasing the compressor pressure ratio π . Especially for the LC cycle, as π is increased from 1.0 to 3.5, T_g drops by 59°C for both considered x_{s0} values, enabling the use of lower temperature driving heat. In the HC cycle, the generator temperature drops by 54 and 49.4°C for $x_{s0}=30\%$ and 40% , respectively.

The cycle circulation ratio CR is defined as the ratio of the strong solution mass flow rate over the refrigerant mass flow rate

$$CR = \frac{m_s}{m_r} = \frac{1 - x_w}{x_s - x_w} \quad (26)$$

Lower circulation ratio is due to the higher refrigeration production rate for the same strong solution mass flow rate, and thus, will lower the system volume size for the same refrigeration output. In the HC cycle, both strong and weak solution concentrations remain constant as the compressor pressure ratio increases, and thus, the refrigeration production remains the same. In the LC cycle, constant refrigeration production is maintained by synchronizing the increase of the strong and weak solution concentrations at the same time, the concentration difference drops slightly. The circulation ratio CR thus remains constant for both cycles.

The performance of the absorption subcycle in the hybrid cycle can be evaluated by the ratio R of distillate (refrigerant) production rate to the generator heat input rate

$$R = m_r/Q_g \quad (27)$$

in which m_r is the distillate (refrigerant) mass flow rate, and Q_g is the heat input rate to the generator.

The variation of R with the compressor pressure ratio is shown in Fig. 4. In the LC cycle, R increases significantly with the pressure ratio, indicating a significant improvement of the absorption subcycle performance. The increasing strong solution concentration along with the increase of pressure ratio improves the generator working conditions, leading to lower heat demand in the generator reboiler for the desorption of the refrigerant, especially at the lower compression ratio region. At the same time, the performance of the mechanical compression deteriorates as the associated power consumption increases. The beneficial gain in the absorption subcycle and the steady increase of power consumption by the mechanical compression have opposite effects on the hybrid cycle COP_p , leading to the existence of an optimal pressure ratio π_{opt} for the hybrid cycle. The LC cycle exhibits higher COP_p , for $x_{s0}=30\%$, its COP_p reaches the highest value of 46% at the optimal pressure ratio of 2.5, which is a 15.2% increase as compared with the pure absorption cycle with $\pi=1.0$. Higher strong-solution concentration is observed to be favorable to increasing COP_p , the optimal value of COP_p with $x_{s0}=40\%$ is found to be 54%, and it occurs at lower pressure ratios of 1.5–2.0.

R varies very mildly with π in the HC cycle, the decrease of generation pressure favors the generation performance but also in a very moderate way, and therefore, the performance of the absorption subcycle increases very slightly and cannot compensate for the concomitant increase of the compressor power consumption, thus leading to the drop of COP_p with pressure ratio.

The analysis shows that the LC cycle delivers a combination of higher COP_p and lower T_g . Along with the increase of the compressor pressure ratio, its concentration difference Δx drops slightly, and the circulation ratio CR remains constant. Consequently, Δx and CR are not good energy performance indicators for the absorption subcycle, contrary to the suggestion by some other studies [4,12,13]. Instead, the absorption subcycle performance is found to be mainly dependent on the generation (rectification) performance, characterized by the parameter R ; and the performance of the hybrid cycle is determined by the interaction

of the two subcycles. This implies an important cycle hybridization principle: the hybridization should promote the thermal compression by improving its rectification process energy performance R , and the energy performance gain from the thermal compression should be higher than its loss from the mechanical compression.

5 Exergy Analysis and Clarification of the Energy Saving Process

5.1 Exergy Analysis. The exergy analysis is conducted with the same assumptions as those in Sec. 4.1. The results are summarized in Table 5. For producing the same amount of refrigeration exergy of 3.38 MW, the comparison absorption cycle (AC) has an exergy efficiency of 28.7% with 97.8% of its exergy input from heat source at a temperature of 151.7°C and 2.2% pump power input. The highest exergy destruction occurs in the generator (GEN) process, which accounts for 23.1% of the total exergy input, followed by 20.3% exergy destruction in the absorber. The vapor compression (VC) cycle has a much higher performance, of $\eta_{ex}=34.9\%$, with 100% input from electricity, and 40% of the exergy destructions occurs in the condensation process.

Comparing the hybrid systems operating in modes LC and HC with the two nonhybrid systems having the same refrigeration production, hybridization is thus shown to allow exergy input of low-temperature heat to decrease significantly due to both the lower heat input quantity and its quality (temperature). This is especially so in the LC cycle, which has the low-temperature input heat exergy of 5.76 MW that is only 50% of the input exergy to the nonhybrid absorption cycle. The thermal exergy input accounts for 62.3% of the total exergy input in the LC mode and 67.8% in the HC mode.

The exergy destruction in the generation process decreases significantly in both hybrid cycles. In the HC mode, the percentage of exergy destruction drops to 11.27% in the generator, as compared with 23.11% in the absorption cycle (AC). The compressor elevates the condensation inlet temperature to 150°C , leading to more heat dumped in the condensation process and a consequent high exergy destruction of 13.5%, which is double that in the nonhybrid absorption cycle. The improvement in the generation process dominates, leading to a higher exergy efficiency, of 32.4%, by 12.7% higher than that of the nonhybrid absorption cycle (AC), which is different from the conclusion of the energy analysis.

In the LC cycle, the reduction of the exergy destruction in the generator (GEN in Table 5) is even more significant, only 4.68% of the total exergy input, lower by 18.4%-points than that in the

Table 5 Comparative exergy analysis

Cycle	Hybrid LC		Hybrid HC		AC		VC	
Exergy input	MW	%	MW	%	MW	%	MW	%
E_g	5.76	62.3	7.08	67.8	11.50	97.8	—	—
W_p	0.245	2.65	0.090	0.86	0.263	2.2	—	—
W_c	3.245	35.1	3.27	31.3	—	—	9.675	100
Exergy output and exergy efficiency								
E_e	3.378	36.5	3.378	32.36	3.378	28.72	3.378	34.92
Exergy destructions in the cycle and its components								
GEN	0.433	4.68	1.176	11.27	2.718	23.11	—	—
CON	0.782	8.46	1.412	13.53	0.783	6.66	3.907	40.4
HEX1	0.374	4.05	0.375	3.59	0.375	3.19	0.368	3.80
V1	0.427	4.62	0.426	4.08	0.427	3.63	0.441	4.56
COMP	0.738	7.98	0.714	6.84	—	—	1.581	16.34
ABS	2.181	23.6	2.378	22.78	2.389	20.31	—	—
P	0.165	1.78	0.030	0.28	0.143	1.21	—	—
HEX2	0.71	7.68	0.5	4.79	1.46	12.41	—	—
V2	0.06	0.65	0.05	0.48	0.09	0.765	—	—
Total	5.87	63.5	7.09	67.64	8.385	71.28	6.297	65.08

nonhybrid absorption cycle (AC). The introduction of the compressor upstream of the absorber also raises its inlet temperature to 134 °C. However, due to the higher weak solution concentration, the absorption heat is even reduced, so is the exergy destruction, which is 2.18 MW in the hybrid cycle as compared with 2.39 MW in the absorption cycle (AC). The hybridization thus improves the exergy efficiency significantly, to of 36.5%, which is higher by 27.2% than that of the nonhybrid absorption cycle.

Comparison of the LC hybrid cycle with the mechanical vapor compression cycle (VC), which has a much higher COP_p , the former consumes only 36% of the electricity consumed by the latter, to produce the same amount of refrigeration. Furthermore, the hybrid cycle accomplishes this significant reduction in electricity consumption by using low-temperature heat, and achieves an exergy efficiency of 36.5%, which is 1.6%-points higher than that of the vapor compression cycle. It is of significant importance that the hybrid cycle with a 62.3% exergy input coming from a low-temperature heat source has a higher exergy efficiency than the electricity-driven mechanical compression cycle.

To quantify this important feature, we define the thermal exergy driven efficiency as:

$$\eta_{ex,th} = \frac{E_{e,h} - E_{e,VC}}{E_g} \quad (28)$$

where $E_{e,h}$ is the refrigeration exergy output from the hybrid cycle, and $E_{e,VC}$ is the refrigeration exergy output of the nonhybrid vapor compression cycle (VC) for the same electricity consumption as the hybrid cycle, $\eta_{ex,th}$ thus represents the refrigeration exergy efficiency obtained from using the thermal exergy input, found to be 37.5% in the LC hybrid cycle, the hybrid cycle can use the low-temperature heat in a much more efficiency way.

The exergy analysis uniquely demonstrates that the hybridization has improved the absorption subcycle performance with significantly reduced generation-associated exergy destruction. The exergy destruction in the absorption and condensation processes still remain high however. Heat recuperation from the absorption process in the LC cycle and from the condensation process in the HC cycle helps to reduce these related exergy destructions.

To summarize, the exergy analysis clearly demonstrates that the hybrid cycle has improved the ability to use low-temperature heat in an efficient way that is not attainable in the absorption cycle and also achieves significant electricity saving as compared with the vapor compression cycle. These important conclusions from the exergy analysis could not have been obtained from energy analysis alone.

5.2 Analysis of the Energy Saving Process in the Hybrid Cycles. Based on the understanding of the performance of the two subcycles of absorption (thermal) compression and vapor (mechanical) compression, the energy saving process of the LC cycle is discussed with the help of $\log P-T$ and $T-h$ diagrams. The absorption cycle (AC) and vapor compression (VC) cycle are also included for comparison, for the same evaporation and condensation parameters.

Figure 6 describes the diagrams of $\log P-T$ of the hybrid (solid line) and absorption cycles (dotted line). Each state point is positioned based on its pressure and temperature. In addition, from left to right, the refrigerant concentration is in a descending order for the phase equilibrium lines ($x_r > x_s > x_w$). The two cycles have the same refrigerant mass flow rate and concentration, and they share the same parameters for the condensation (represented by paths 2–3), precooling (3–4), throttling (4–5), and evaporation processes (5–6), and heat exchanging (6–7). The main difference between the hybrid and absorption cycles is the existence of the compression process (7–7') in the former, which elevates the absorption pressure from the evaporation pressure of 1.55 bar (point 7) to the higher level of 3.8 bar (point 7'). Therefore, the

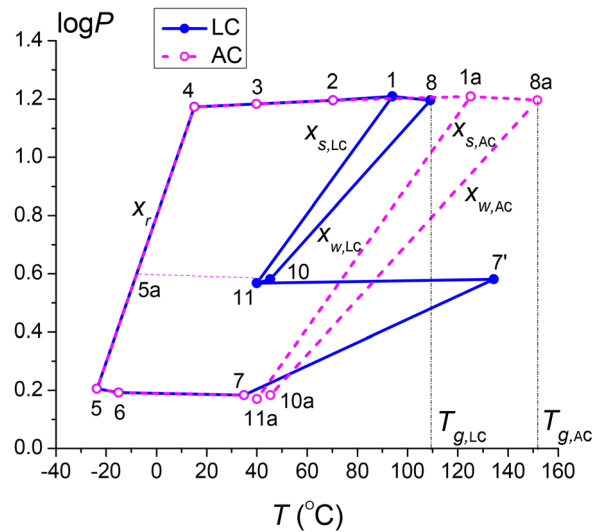


Fig. 6 Log $P-T$ diagram for the hybrid LC and the nonhybrid AC cycles

absorption subcycle (thermal compression) only manages further boosting of pressure to the generation pressure of 15.7 bar (point 1). The absorption in the hybrid cycle is 7'/10–11 for the hybrid cycle as compared with 7/10a–11a for the absorption one.

The generation process occurs at the same pressure of 15.7 bar for both hybrid and absorption cycles, as 1–2/8 for the hybrid and 1a–2/8a for the absorption one. It is observed that both strong and weak solution concentrations in the hybrid cycle are higher than those in the absorption cycle, i.e., $x_{s,LC} > x_{s,AC}$, and $x_{w,LC} > x_{w,AC}$, leading to significant decrease ($>40^\circ\text{C}$) of the generation temperature, to 109°C in the hybrid cycle. Furthermore, also the amount of the generation heat use decreases since it generates refrigerant from a higher concentration solution at point 1, as compared to 1a in the absorption cycle.

It is also noteworthy that the temperature of refrigerant corresponding to the absorption pressure of 3.8 bar is -3°C , so a nonhybrid absorption cycle driven by the low-temperature heat of 109°C can produce refrigeration at a temperature of -3°C (shown as state point 5a in Fig. 6). Further refrigeration down to -23°C is accomplished in the compression subcycle, which the nonhybrid absorption cycle would have attained only if operated at a much higher heat source temperature, of 152°C . Meng et al. [13] referred to this hybridization as “cascade refrigeration,” which not only enables the refrigeration to be produced beyond what is attainable in the absorption cycle, but also reduces its heat demand quality and quantity.

Figure 7 describes the $T-h$ diagrams of the hybrid (solid line) and the vapor compression (dashed line) cycles.

The comparison is based on the same evaporation and condensation pressure and temperature, and the same refrigerant mass flow rate. In the hybrid cycle, the refrigerant loop is 2–3–4–5–6–7–7'–2, and the solution loop is 1–8–9–10–11. The vapor compression cycle is represented by 2–3–4–5–6–7–7'a–2. The two cycles have therefore the same evaporation process (paths 5–6), from which they produce the same amount of refrigeration at -23°C . At the exit of the evaporator, the vaporized refrigerant is compressed directly to the condensation pressure in the VC cycle (path 7–7'a). In the hybrid cycle, the vaporized refrigerant (7) is pumped to the absorption pressure (7–7'), and then is absorbed by the weak solution (10) to form the strong solution (11). The length of projection of each process line onto the h -axis denotes the enthalpy change of the process. The projection length of the compression process (path 7–7') represents therefore the mechanical work consumption in the hybrid cycle $W_{c,LC}$, while that of the compression process 7–7'a represents the

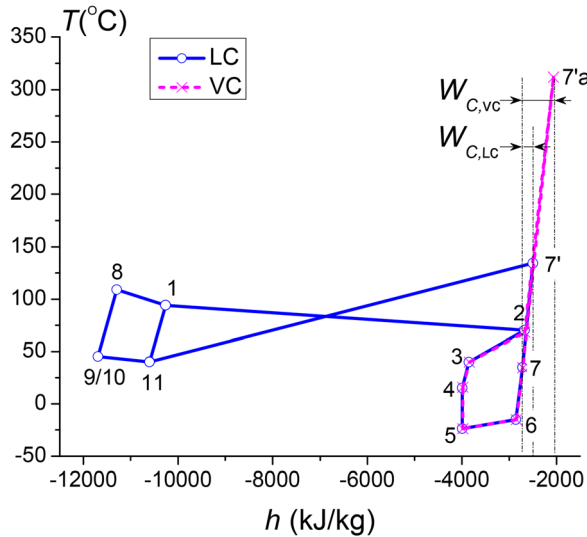


Fig. 7 T - h diagram for the hybrid LC and the nonhybrid VC cycles

mechanical work consumption $W_{C,VC}$ in the VC cycle. Obviously, the former is only 1/3 of the latter. The rest of the input comes from the low-temperature heat source of 109 °C (point 8). It is assumed in this study that the compressors have the same isentropic efficiency, but in fact the compressor in the VC cycle with the higher compression ratio and higher discharge temperature generally has a lower efficiency, leading to additional power consumption. Based on the data in Table 4, the electricity consumption in the hybrid cycle is 3.49 MW to produce 17 MW refrigeration at -23 °C. The electricity consumption increases to 9.68 MW to produce the same amount of refrigeration in the VC cycle. The mechanical work saving ratio defined in Eq. (29) of the hybrid cycle is 64%

$$ESR = \frac{W_{VC} - W_h}{W_{VC}} \quad (29)$$

It is concluded that replacement of a part of the mechanical compression with thermal compression, enables the hybrid cycle to achieve significant energy saving of mechanical work.

6 Conclusions

The absorption-compression hybrid refrigeration cycle type was studied, focused on a hybridization principle based on the interrelation between the two subcycles, and the resulting energy saving processes were analyzed. The theoretical analysis was validated by a simulation of a hybrid cycle working with $\text{NH}_3/\text{H}_2\text{O}$ solution.

To explore the thermodynamic performance and the energy saving process of the hybrid system, both energy and exergy approaches were used to conduct a comparison among the hybrid cycles and the nonhybrid absorption refrigeration cycle (AC) and the nonhybrid vapor compression cycle (VC), which work within the same temperature regions. It was found that the LC cycle (with a low-pressure-side compressor, and reduced generation temperature) offers the best performance in exhibiting both higher COP and lower driving heat temperature. The hybridization resulted in a 50–60 °C decrease in the needed generation temperature (T_g) by increasing the compressor pressure ratio from 1.0 to 3.5, COP_p increases by up to 15% (without internal heat recuperation) as compared with the nonhybrid absorption cycle. To produce the same amount of refrigeration, the hybrid LC cycle achieves an exergy efficiency of 36.5%, which is 27% higher than the nonhybrid absorption cycle, and 4.5% higher than the nonhybrid vapor compression cycle, achieving a thermal-driving exergy

efficiency of 37.5% and mechanical work saving ratio reaches up to 64%.

The compression in the hybrid cycle can be regarded as a combination of mechanical compression and thermal compression. The hybridization enhances the refrigeration ability of the low-temperature heat input in a way that not only enables the refrigeration to be produced beyond what is attainable in the absorption cycle, but also reduces its heat demand quality and quantity. The interrelation between the two subcycles determines the hybrid cycle performance and the existence of the optimal compressor compression ratio. The hybridization principle was therefore proposed to promote the absorption-based thermal compression by improving its generation process and to make the gain from the thermal compression side higher than the loss from the mechanical compression side.

It was concluded that replacement of a part of the thermal compression by mechanical compression causes the hybrid cycle to achieve significant saving of mechanical work (high-quality energy), and also improves the low-temperature thermal compression performance to a level which cannot be achieved in a nonhybrid absorption refrigeration cycle, i.e., it achieves simultaneously better use of low-temperature waste heat and energy saving of mechanical work attributed to the thermodynamically efficient cascade use to the two energy inputs.

Acknowledgment

The authors gratefully acknowledge the support of the National Key Fundamental Research Project of China (Grant No. 2014CB249202) and the National Natural Science Foundation of China (Grant No. 51236008).

Nomenclature

COP_0 = the first law coefficient of performance, dimensionless (Eq. (21))

COP_p = primary energy-based coefficient of performance, dimensionless (Eq. (22))

CR = cycle circulation ratio, dimensionless (Eq. (26))

E = exergy, MW

ESR = electricity (mechanical work) saving ratio (Eq. (29))

h = specific enthalpy, kJ/kg

m = mass flow rate, kg/s

P = pressure, bar

Q = heat duty, MW

R = (refrigerant production rate)/(generator heat input rate), kg/MJ (Eq. (27))

s = specific entropy, kJ/kg K

T = temperature, °C

W = power consumption, MW

x = solution concentration, kg/kg

Δx = solution concentration difference, kg/kg

Greek Symbols

η_e = electricity generation efficiency

η_{ex} = exergy efficiency (Eq. (23))

$\eta_{ex,th}$ = heat driven exergy efficiency (Eq. (28))

π = compressor pressure ratio, dimensionless

Subscripts

a = absorber

AC = absorption cycle

c = condenser, compressor

e = evaporator

g = generator

h = hybrid cycle

opt = optimal value

p = pump

r = refrigerant

s = strong solution
VC = vapor compression cycle
 w = weak solution

References

- [1] Fan, Y., Luo, L., and Souyri, B., 2007, "Review of Solar Sorption Refrigeration Technologies: Development and Applications," *Renewable Sustainable Energy Rev.*, **11**(8), pp. 1758–1775.
- [2] Ayala, R., Heard, C. L., and Holland, F. A., 1997, "Ammonia/Lithium Nitrate Absorption/Compression Refrigeration Cycle. Part I. Simulation," *Appl. Therm. Eng.*, **17**(3), pp. 223–233.
- [3] Kim, J. S., Ziegler, F., and Lee, H., 2002, "Simulation of the Compressor-Assisted Triple-Effect H₂O/LiBr Absorption Cooling Cycles," *Appl. Therm. Eng.*, **22**(3), pp. 295–308.
- [4] Boer, D., Valles, M., and Coronas, A., 1998, "Performance of Double Effect Absorption Compression Cycles for Air-Conditioning Using Methanol-TEGDME and TFE-TEGDME Systems as Working Pairs," *Int. J. Refrig.*, **21**(7), pp. 542–555.
- [5] Ventas, R., Lecuona, A., Zacarias, A., and Venegas, M., 2010, "Ammonia-Lithium Nitrate Absorption Chiller With an Integrated Low-Pressure Compression Booster Cycle for Low Driving Temperatures," *Appl. Therm. Eng.*, **30**(11–12), pp. 1351–1359.
- [6] Kang, Y. T., Hong, H., and Park, K. S., 2004, "Performance Analysis of Advanced Hybrid GAX Cycles: HGAX," *Int. J. Refrig.*, **27**(4), pp. 442–448.
- [7] Kumar, A. R., and Udayakumar, M., 2007, "Simulation Studies on GAX Absorption Compression Cooler," *Energy Convers. Manage.*, **48**(9), pp. 2604–2610.
- [8] Kumar, A. R., and Udayakumar, M., 2008, "Studies of Compressor Pressure Ratio Effect on GAXAC (Generator-Absorber-Exchange Absorption Compression) Cooler," *Appl. Energy*, **85**(12), pp. 1163–1172.
- [9] Hong, D., Tang, L., He, Y., and Chen, G., 2010, "A Novel Absorption Refrigeration Cycle," *Appl. Therm. Eng.*, **30**(14–15), pp. 2045–2050.
- [10] Chen, G., and Hihara, E., 1999, "A New Absorption Refrigeration Cycle Using Solar Energy," *Sol. Energy*, **66**(6), pp. 479–482.
- [11] Han, W., Sun, L., Zheng, D., Jin, H., Ma, S., and Jing, X., 2013, "New Hybrid Absorption-Compression Refrigeration System Based on Cascade Use of Mid-Temperature Waste Heat," *Appl. Energy*, **106**, pp. 383–390.
- [12] Zheng, D., and Meng, X., 2012, "Ultimate Refrigerating Conditions, Behavior Turning and a Thermodynamic Analysis for Absorption-Compression Hybrid Refrigeration Cycle," *Energy Convers. Manage.*, **56**, pp. 166–174.
- [13] Meng, X., Zheng, D., Wang, J., and Li, X., 2013, "Energy Saving Mechanism Analysis of the Absorption-Compression Hybrid Refrigeration Cycle," *Renewable Energy*, **57**, pp. 43–50.
- [14] Heller, L., and Farago, J., 1955, "Absorption Refrigeration at Very Low Temperatures," IX Congress International Institute of Refrigeration, Vol. 1, Paris, France, Paper No. 3203.
- [15] Aspen Technology, Inc., 2012, "Aspen Plus," Version 7.3, Aspen Technology, Burlington, MA, accessed Sept. 2016, <http://www.aspentech.com/>
- [16] International Institute of Refrigeration, 1994, "Thermodynamic and Physical Properties NH₃-H₂O," International Institute of Refrigeration, Paris.
- [17] Zhang, N., and Lior, N., 2007, "Methodology for Thermal Design of Novel Combined Refrigeration/Power Binary Fluid Systems," *Int. J. Refrig.*, **30**(6), pp. 1072–1085.
- [18] Zhang, N., and Lior, N., 2007, "Development of a Novel Combined Absorption Cycle for Power Generation and Refrigeration," *ASME J. Energy Resour. Technol.*, **129**(3), pp. 254–265.
- [19] Lior, N., and Zhang, N., 2007, "Energy, Exergy, and Second Law Performance Criteria," *Energy*, **32**(4), pp. 281–296.